LAWRENCE
LIVERMORE
NATIONAL
LABORATORY

LLNL-PROC-425270

Deflagration Rates and Molecular Bonding Trends of Statically Compressed Secondary Explosives

J. M. Zaug, M. F. Foltz, E. Hart

March 9, 2010

14th International Detonation Symposium
Coeur d'alene, OR, United States
April 11, 2010 through April 16, 2010

Disclaimer

Deflagration Rates and Molecular Bonding Trends of Statically Compressed Secondary Explosives

Joseph. M. Zaug[a], M. Frances Foltz[a], and Elaine K. Hart[b]

[*]Lawrence Livermore National Laboratory,
Physical Life Sciences, Livermore, California 94551

[b] Stanford University, Civil and Environmental Engineering Department, Palo Alto, California 94305

Abstract. We discuss our measurements of the chemical reaction propagation rate as a function of pressure. Materials investigated have included CL-20, HMX, TATB, and RDX crystalline powders, LX-04, Comp B, and nitromethane. The anomalous correspondence between crystal structure, including in some instances isostructural phase transitions, on pressure-dependant RPRs of TATB, HMX, Nitromethane, CL-20, and PETN have been elucidated using micro-IR and -Raman spectroscopies. Here we specifically highlight pressure-dependent physicochemical mechanisms affecting the deflagration rate of nitromethane and epsilon-CL-20. We find that pressure induced splitting of symmetric stretch NO_2 vibrations can signal the onset of increasingly more rapid combustion reactions.

Introduction

Knowledge of high-pressure chemistry is fundamental toward understanding combustion and detonation processes. Diamond-anvil cell (DAC) reaction propagation rate (RPR) results, combined with strand burner measurements below 1 GPa, are important to understanding processes such as deflagration-to-detonation transition (DDT), thermal explosion (and its associated violence), sympathetic detonation, and buildup of reaction following impact ignition, and generally assist in assessing potential outcomes of accident scenarios.

We find that the deflagration rates of pre-compressed explosives and polymer-blended explosives never exhibit purely monotonic pressure dependence. While materials studied to date have included a wide variety of materials (crystalline powders CL-20, HMX, TATB, and RDX, energetic liquid Nitromethane, explosive mixtures LX-04[a], Composition B[b]), here we limit discussion to two very different systems: epsilon phase CL-20 and nitromethane (NM). We consider how discontinuities observed in pressure-dependent vibrational spectra e.g., IR, Raman, may signal the onset of deflagration rate changes and/or product formation.

Experimental Procedure

Deflagration rates were determined from materials pre-compressed to > GPa pressure within a diamond-anvil cell. Sample preparation, pressure measurement and deflagration measurement methods have been discussed elsewhere.[1,2] The experiment consists of back illuminating a sample pressurized in a DAC (no additional medium),

[a] 85% HMX and 15% Viton A binder
[b] 63% RDX, 36% TNT, 1% wax

with several Watts of coherent visible light from an argon ion laser. The light transmitted through the sample generates a speckle pattern that is mapped onto the slit of a streak camera. A second pulsed laser is employed to initiate a reaction in the center of the sample. Dense or optically opaque and hot reaction product gases mask the original speckle pattern. The disappearance of the speckle pattern across a time-streaked micrograph provides a direct measurement of the speed of the deflagration wave.

Static pressure mid-IR Fourier transform infrared (FTIR) spectra of CL-20 polymorphs and NM single crystals were taken over the pressure range of 0.3–13 and 1-38 GPa respectively using either a benchtop Nicolet System 730 or a Bruker Vector-33 interferometer (4000-550 cm^{-1}, 4 cm^{-1} resolution, 32 scans). CL-20 micro-pellets were prepared by first pressing KBr (with embedded ruby-chip manometers) to transparency within a drilled metal gasket, then pressing a thin layer of explosive on top of the KBr "window".[1] KBr was included to reduce signal saturation. For NM, single crystals were grown within an argon pressure medium by moderating temperature at a near constant pressure of 1 GPa. Crystal growth was terminated when the desired sample thickness was achieved by using IR absorption of the most intense spectral peaks as feedback.

Results

CL-20

Pressure dependent mid-IR spectral trends and reaction propagation rate data for α, β, γ, and ε polymorphs of CL-20 have been previously published.[3] Data for ε-CL-20 is reproduced in Figure 1 (line through the data points is a guide for the eye). Infrared spectra showed changes in the intensity, width and frequency position of peaks with increasing pressure. Two regions of these spectra are emphasized: the C-H stretch (3200-3000 cm^{-1}) and the ring + NO_2 deformation modes (700-830 cm^{-1}). Higher pressure RPR data were subsequently obtained for the four polymorphs, specifically α-CL-20 to ~35 GPa, β-CL-20 to ~24 GPa, γ-CL20 to ~32 GPa, and ε-CL20 to ~27 GPa. The RPR data for ε-CL-20 is shown in Figure 2.

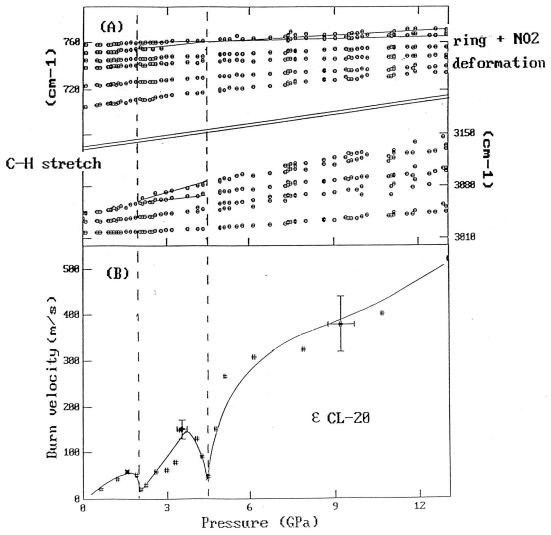

Fig. 1. (A) Mid-IR static pressure-induced spectral changes correlated with (B) reaction propagation rate inflections of ε-CL-20.

Superimposed on the plot are pressure regimes identified by Ciezak et al. as corresponding to pressure-induced phase transitions identified from mid-IR spectral data.[4] While all four polymorphs exhibit consistent RPR performance up to ~12.5 GPa, burn rates between 12.5-19 GPa of three are erratic ranging from 200 m/s to ~1260 m/s (β-CL-20 erratic burn rate region is shifted to 17-25 GPa). Above 20 GPa RPR rates are more erratic than at low pressure but follow the same general upward trend. We note that Ciezak employed a helium pressure medium, which imparts far less shear forces to the sample. Consequently their intermolecular transitions will, and do, occur at higher pressures than inflections seen in the RPR.

Anomalous ignition sensitivity through specific pressure regimes may indicate highly stressed transitional states. For example, for the γ-polymorph we found that unless the sample was pre-compressed to ~5-7 GPa accidental ignition occurred 50% of the time with either the defocused back lighting argon ion laser (514.5 nm, ~15 kW/cm^2) or the low energy alignment pulsed laser beam. This is a surprising result since the RPR data for gamma and alpha CL-20 are otherwise nearly identical up to 30 GPa.

RPR data between 8-9 GPa for β-polymorph

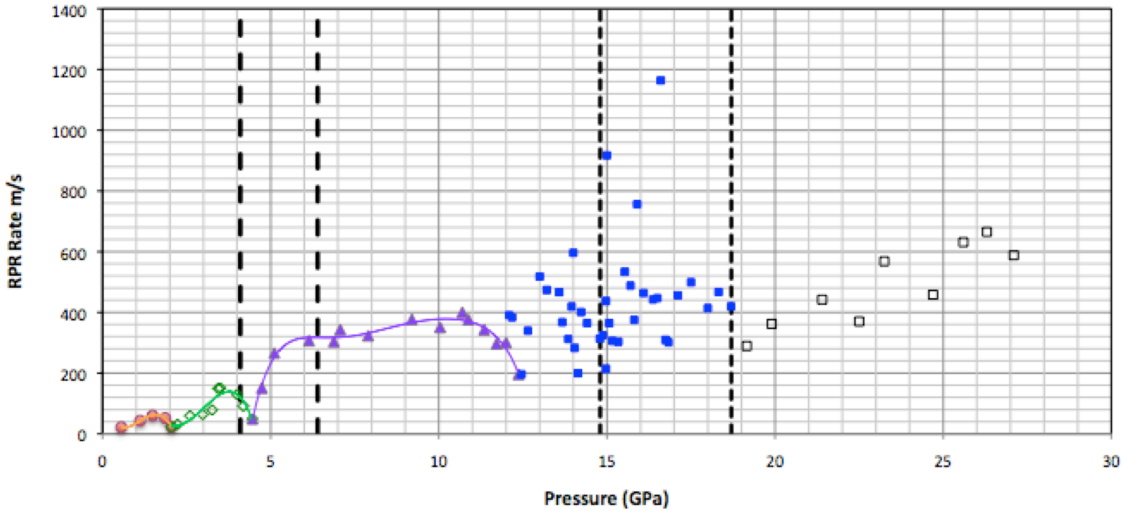

Fig. 2. Reaction propagation rate data for ε-CL-20. Dashed lines bracket two polymorphic phase conversions identified from mid-IR spectra by Ciezak, et al. (Ref. 4).

were also difficult to obtain due to similar sensitivity to accidental photo ignition. Otherwise the RPR for β-CL-20 mimics that of ε-CL-20 by going through the same inflections at 2 GPa and 4.5 GPa, but diverges above 9 GPa.

Nitromethane

Previously published RPR data from NM are presented in Figure 3.[5] Four distinct regions are marked where an acceleration or deceleration of rate occurs and/or the decomposition product changes phase and color. NM exhibits varying degrees of pressure dependent photosensitivity, which may be cause for concern when attempting to collect Raman data. Normally DAC IR data are collected over a large spatial domain e.g., 30-100+ μm; consequently many different crystallographic orientations can be sampled simultaneously - IR peak fidelity is degraded. Recently we collected micro-IR data on three different single crystals of NM with intent to overcome both issues. Here we present selected NM mid-IR absorbance contour data (298 K) from one crystal (Figure 4 a,b.). The instrument was described previously.[6] Two of three RPR inflection points can be linked to changes in these vibrational spectra, (I-II) a sharp discontinuity in CH_3 and NO_2 vibrational intensity at 4-5 GPa and, (II-III) a market drop in CH_3 deformation population, a splitting of the symmetrical NO_2 stretch, a partial termination of the asymmetric NO_2 stretch, and a significant increase in the C-H stretch vibration population. We note again that the softer argon pressure medium inflicts much less shear strain compared to pure crystalline NM. And note that this difference only becomes manifest for the highest infection pressure point (III-IV).

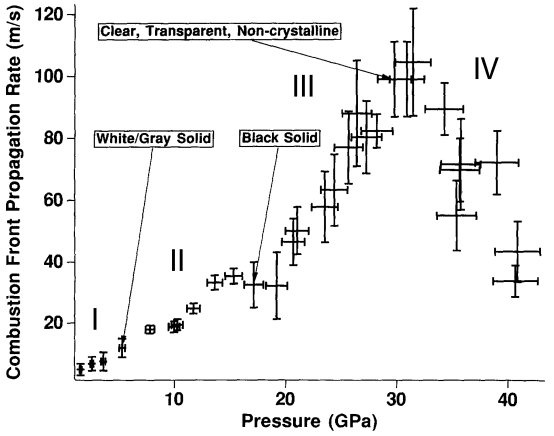

Fig. 3 Reaction propagation rates from precompressed and photoinitiated nitromethane, with permission from Rice and Foltz, 1991.[5]

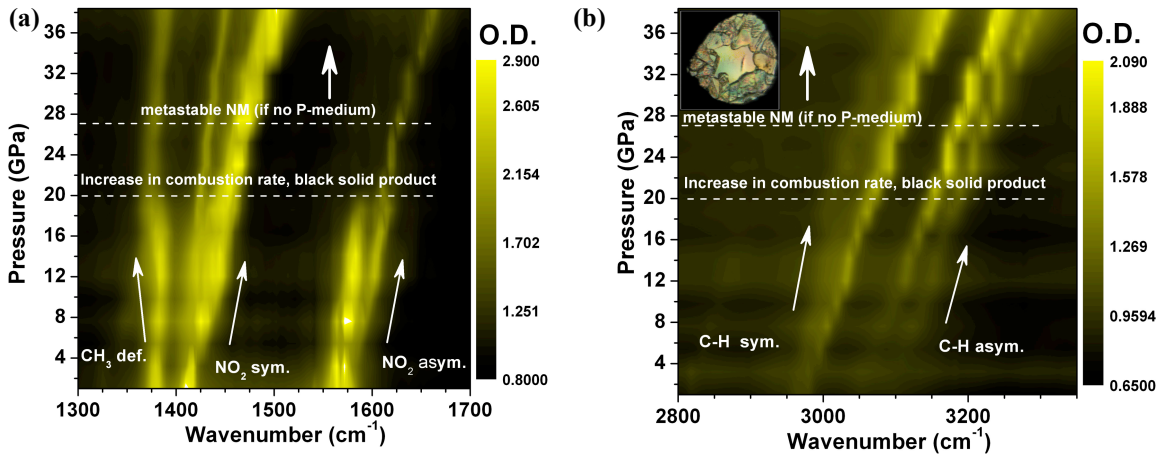

Fig. 4. FTIR absorption contour plots of (a) CH_3 deformation and NO_2 stretch regions (b) C-H stretch region from a single NM crystal. The inset photomicrograph (NM at 31.5 GPa) was taken under cross-polarized light. The clear central region is pure argon. The cavity is 220-240 μm across and <10 μm thick.

Discussion

CL-20

Ciezak et al. also examined the high-pressure response of ε-CL-20 in a DAC with helium pressure medium up to ~27 GPa using both Raman and FTIR vibrational spectroscopy. [4] Their Raman data suggests two phase transitions, the first sluggish transition starting at ~4.1GPa and ending at 6.5 GPa (proposed ε→γ). A second sluggish phase transition begins near 14.8 GPa and doesn't complete until 18.7 GPa (proposed γ→ζ). They note that the most apparent modification in the Raman spectra at pressures above 14.8 GPa occurs in the C-H stretching region where four modes merge into three broad peaks. The pressure-induced shifts in their FTIR data suggest a phase transition between 4.1 and 6.9 GPa - the intensity of the 650 cm^{-1} C-N-C stretching band increasing nearly two-fold between 4.1-6.9 GPa, and the two NO_2 torsional modes collapsing into a single broad peak near 6.9 GPa. Near 18 GPa they report slight discontinuities in frequency shifts and dν/dP decreases, which indicates either a distortion within the unit cell or the onset of structural phase transition.

Gump et al., investigated the crystal structure of powdered ε-CL-20 using synchrotron angle-dispersive x-ray diffraction and Raman spectroscopy (50-1650 cm^{-1}). [7] X-rayed samples were compressed under hydrostatic and non-hydrostatic conditions to 6.3 GPa; the spectroscopy samples were compressed non-hydrostatically to 7.1 GPa. No phase transitions were observed within this pressure regime.

Russell et al. had previously identified a rapid and reversible room temperature pressure-induced γ→ζ transition in CL-20 at 0.7 ± 0.05 GPa. [8] Work presented here did not thoroughly probe this low-pressure regime but a probable transition seen at 1.4 GPa (inflection in RPR, changes in mid-IR spectra) likely signals this transformation. Conformation of a corresponding polymorph has not been reported.

The non-planar CL-20 molecule consists of an isowurtzitane cage surrounded by six NO_2 groups appended to six nitrogen atoms in the cage (Figure 3). The known stable polymorphs (ambient conditions) differ by orientations (*endo* or *exo*) of the NO_2 groups with respect to the 5-membered imidazolidine and the boat-shaped 6-membered pyrazine rings (Table 1). [9] Designators Y and N indicate the conformer is/is not allowed by symmetry; dash indicates a redundant structure; * designates the more sterically stable structures. [c]

[c] While the gamma and alpha polymorphs have the same molecular conformation, packing differently

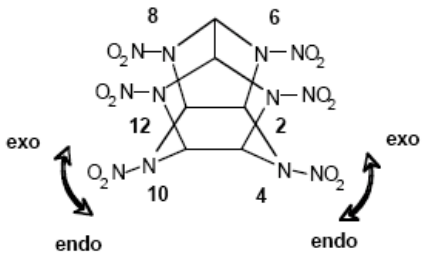

Fig. 5. Numbering of CL-20 nitramine locations and orientation of the two NO_2 groups with respect to the six-membered ring as noted in Table 1.

Observed pressure-induced changes in the C-H stretch and ring + NO_2 deformation modes indicate reorientation of the NO_2 groups about the relatively rigid molecular cage structure. The intensity change in the C-N-C stretch and merging of the NO_2 torsional modes (Ciezak et al.) indicate a structural modification of the NO_2 geometry.

That reorientation of the nitro groups about the isowurtzitane cage is the dominant mechanism behind inflections in the RPR curve is supported by the behavior of the α- and γ-polymorphs. These two polymorphs have the same molecular conformation but fill different unit cell lattices. In addition the alpha crystal lattice is stabilized by H_2O in the unit cell with 17-50% cavity occupancy. The relative insensitivity of the α-polymorph may be due, in part, to the presence of water trapped within the unit cell.

Not all phase transitions involve re-packing molecules in the crystal lattice. For example, displacive transformations occur with great rapidity because nearest neighbors remain as such, thus rendering intermolecular bonds intact.[10] In this example, there is little difference in energy content between the high and low polymorphs. Gump et al. observed only unit cell contraction with no x-ray evidence to support the notion of a

Table 1. Top views of the conformers of CL-20

Polymorph (N-10) - (N-4) Orientation				
Structure	**exo-exo**	**exo-endo**	**endo-exo**	**endo-endo**
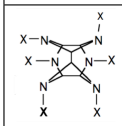	α * γ *	Y *	Y *	N
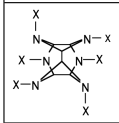	β *	Y *	–	N
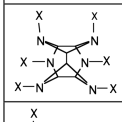	Y *	ε *	–	N
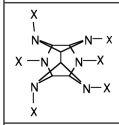	Y *	Y	Y *	N
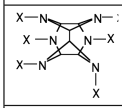	Y *	Y *	Y	N
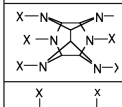	Y	Y	–	N
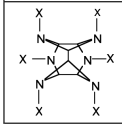	Y *	Y	–	N

phase change up to 6.2 GPa. These claims are consistent with a slight reorientation of nitro groups about the isowurtzitane cage occurring as the molecules are compressed together. Mid-IR spectral evidence supports this hypothesis. Reorientation of NO_2 units would seem to be a plausible low-energy and likely reversible mechanism.

Regarding the anomalous high photo sensitivity of β-CL-20 between 8-9 GPa, we note that the crystal structure of this polymorph falls in the non-centrosymmetric orthorhombic class point group mm2 (space group $Pb2_1a$).[11] This class is piezoelectric and optically active with hydrostatic, compression, and torsion piezoelectric moduli. Others have noted the relationship between piezoelectric properties and sensitivity. Raha and Chhabra studied the development of static electric charge resulting from compression of PETN

---

into the crystal lattice, the epsilon polymorph has been incorrectly cited in the literature as being different from the α/γ conformer by the orientation of only one nitro group. They also differ by the orientation of one nitro group on the 6-membered ring.

crystals.[12] PETN belongs to an optically active tetragonal class point group $\bar{4}2m$ ($P\bar{4}21c$ space group) that is piezoelectrically responsive to torsion. It is possible that while the changes in β-CL-20 RPR at 2 and 4.5 GPa correspond to reorientation of the nitro groups on increasingly crowded molecules, the high photosensitivity at 8-9 GPa is caused by a change in crystal structure.

Nitromethane

There have been numerous pressure and temperature dependent studies of the vibrational modes and bonding structures of NM and the results have bootstrapped additional computational efforts. A review of relevant research highlights, within the context of NM RPR results by Rice and Foltz, may yield useful concepts to construct, at the very least, a cursory understanding of how secondary explosive deflagration rates may be affected, controlled, or predicted by structural rearrangements. To begin we focus on each of the four trends made apparent by the RPR study.

Region-one (R1; < 3.5 GPa): one of three intermolecular O--H bond lengths decreases from 2.56 Å to 1.63 Å (T = 4 K) going from ambient pressure to 3.5 GPa, (a staggered molecular confirmation results).[14] Generally the collapse of a covalent bond to one that is equivalent in range with atomic van der Waals interaction radii (carbon vdWr = 1.7 Å) signifies the onset of chemistry.[15] At ambient temperature and 3.0 - 3.5 GPa there is a two-fold jump in the $\nu_a(NO_2)$ Raman peak-width; a phenomena sometimes attributed to enhanced local disorder.[16] Below 2.5 GPa NM is chemically robust when subjected to a photo-excitation pulse (λ_E = 532 nm, 0.33 GW/cm^2). Here combustion products appear as an oily white solid.[5]

Region-two (R2; 3.5-12 GPa): Methyl-group librational dynamics about their equilibrium positions (298 K) are essentially arrested by 7.0 GPa and by 5.4 GPa the pressure-dependent torsional angle inflection (with respect to the N-O_2 plane) reaches >80 % of the terminable value.[17,18] Interestingly, RPR streak micrographs taken in this precompression regime clearly reveal a prewave front: we speculate that this bifurcated deflagration event reveals a two-stage reaction that is common to metalized propellants, e.g., ignition followed by a dark-region followed by combustion.[19] Pressure-induced methyl group rotation leads to an eclipsed molecular confirmation, which enhances O--H attraction and minimizes N--H repulsion. We suggest that this transition from rotationally disordered to eclipsed conformations resembles a sluggish isostructural phase transition; a partially hindered plastic material changing to a rigid crystalline framework. Additionally, static compression to 7.5 GPa leads to an abrupt 1.9% collapse in the $\nu_a(NO_2)$ mode position and a 60% loss in peak-width, which reveals both a weakening and enhanced ordering of the N-O framework.[16] In fact, numerous vibrational mode splittings occur near 7.5 GPa - all suggestive of structural alterations in the face of x-ray data, which confirm no change to the orthorhombic $P2_12_12_1$ symmetry group. Methyl group rotations cease at 11.0 – 12.0 GPa. Concerning the C-N bond: the vibrational modes beginning at 671 cm^{-1} and 936 cm^{-1} are assigned to CN stretching + NO_2 bending. The lower frequency combination begins to split at 7.5 GPa and the higher frequency at 11 GPa. Neither branch softens with pressure. These frequency splittings presumably correspond with the cessation of CH_3 librations and associated modifications to the NO_2 network. Beginning at 6-7 GPa, DAC deflagration products turn solid with a grey color.[5]

Region-three (R3; 10-20 GPa): One of three intermolecular O--H bond lengths (298 K) decreases from 1.92 Å to 1.34 Å with compression from 10.0 to 19 GPa.[14] Citroni et al., proposed (and here we paraphrase) that their degrading x-ray scattering intensities e.g., a 70 % loss of Bragg diffraction peaks, from 14.9 to 16.9 GPa, signal a collapse of local and/or medium-range order, perhaps accounting for a crystalline to amorphous phase transition.[20] It appears that, like ambient pressure thermal decomposition, slow cold-compression induces intramolecular rearrangements prior to irreversible decomposition of NM.[21] This conclusion is congruent with the lack of changes observed in the low frequency phonon modes reported by Lucarré et al. and also the MD shock chemistry results of Manaa et al., however, experimental confirmation of proton abstraction mechanisms occurring near C-J conditions on ultrafast time scales remains

daunting.[23] Above 11.0 GPa a hydrogen bond network develops and seems to stabilize the eclipsed conformation.[20] When applied static pressure nominally reaches twice the bulk modulus of NM, 16.6 GPa, single crystals (no pressure external pressure medium) are turned into powder. In our FTIR study of NM single crystals, the relative population of hydrogen bonding becomes quite pronounced as evident by the market jump in C-H stretch peaks and intensities between 20 and 38 GPa (Figure 4b, see also Ref. 14). Furthermore we note that compressing single crystals of NM (298 K) within an argon matrix i.e., less shear strain relative to no pressure medium, extends the stability field by at least 11 GPa for up to at least several hours. Beginning at 18-19 GPa, the burn rates become significantly more erratic now creating solid black products implying more complete combustion.[5] Moreover the burn rate exhibits a steepening pressure dependence.

Region-four (R4; > 20 GPa): Static compression of NM, (180 – 22 ˚C; 17 -50 GPa) initiates an irreversible crystalline to amorphous phase transition.[23] At ambient pressure the transition is sluggish thus accounting for disparity in reported threshold transition pressures, 25-35 GPa. In the absence of a pressure medium the ambient temperature decomposition reaction slowly begins at 27 GPa and continues above 50 GPa: recovery and IR analysis of a polymeric material indicates the formation of a hydrogen bonded network with similar spectral features to the high-pressure –temperature decomposition product of formic acid.[6,25] The argon pressure medium clearly delays the transition. Therefore we propose that increasing shear forces, intrinsic to the DAC cold compression technique, act to overcome the intermediate-pressure NM hydrogen bond network and thereby shift the intermolecular energy landscape to favor production of a disordered system. The collapse of long-range structural order is associated with a steep decline in the deflagration rate of NM.

Conclusions and Summary

The existence and identification of phase conversions in CL-20 and NM correlated with changes in burn (combustion) rate can be used to explain anomalous shock initiation behavior seen at various laboratories. If the rate of conversion is rapid and an appreciable degree of conversion happens at or immediately behind the shock front, this would cause the unexpected low shock sensitivity of CL-20. Wilson, et al. hypothesized that there may be a phase transition during shock loading that plays a role in apparent shock sensitivity.[25] The material exhibited an anomalous reversal in slope of shock sensitivity vs. input strain. Over limited applied strain, and near the first reaction threshold, the level of reaction was found to decrease.

Shock-induced decomposition of nitromethane may be attributed to four or more mechanisms, 1) aci-ion formation, 2) bi- or multi-molecular (solid-state like) mechanisms, 3) pressure-dependant structural changes, and 4) the formation of transient semimetallic states. The concentration of the aci-ion of nitromethane has been shown to increase with increased pressure and the concentration of amines.[26-28] Correspondingly the reaction sensitivity increases, and therefore aci-ion formation has been suggested as a rate-controlling step in the decomposition mechanism.[29] Previous experimental evidence suggests that there are strong intermolecular interactions accountable for decomposition reaction.[30] This account lead to a molecular dynamics study of bi- and multi-molecular collisions of NM (6.5 – 12.0 km/sec).[31] For low velocity impacts only C-N scission is observed (7 km/sec threshold) where bimolecular simulations only yield fragmentation patterns at high collision velocities; multi-molecular impact simulations reveal more complicated fragmentation patterns, including tri-molecular interactions where the activation barrier for C-N scission is the most dominant reaction coordinate. Molecular dynamic simulations by Manaa et al. expose a tri-molecular proton-abstraction sequence that precedes aci acid, H_2CNO_2H, and aci ion, $H_2CNO_2^-$ formation near the fully reacted Chapman-Jouget condition (T = 3000 K, $\rho = 1.5\ \rho_o$).[22] These authors suggest that C-N scission, as a first decomposition step, is only important for low density thermal reactions such as those reported by Shaw et al.. The cold compression vibrational studies including those presented here seem to bear this supposition out. Concerning the third mechanism listed above, several studies have claimed that NM decomposes

more readily with increased pressure and also with a strong dependence on crystal orientation with respect to an incoming shock wave. According to J. J. Dick, the application of pressure along the <001> direction results in enhanced sensitivity to decomposition.[32] Dick proposed a steric-hindrance model to account for his results. The work of Conroy et al., using an empirical van der Waals correction to their density functional theory (DFT) corroborated the findings of Dick.[33] DFT results indicate that purely uniaxial compression along either the <111> or <001> axes would enhance the shock sensitivity of NM.

The question as to weather NO_2 stretch vibrations telegraph inflections in RPR data we reiterate the following (i) the second RPR inflection of ε-CL-20 is clearly delineated, making allowance for the difference in pressure media, by an energy shift and splitting of NO_2 symmetric stretch vibrations. The combustion rate then jumps nearly 120% over just 1 GPa. Given the lack of nonhydrostatically compressed CL-20 vibrational data, perhaps nothing more can be solidly confirmed; (ii) changes in recovered NM products occurring at approximately 7 GPa correspond with a weakening and enhanced ordering of the N-O framework; (iii) 20 GPa marks a point where the NM RPR trend increases and this is accompanied by a much more pronounced splitting of the NO_2 symmetric stretch. Symmetric NO_2 mode splitting may signal a rise in combustion rate. In addition the NO_2 asymmetric stretch reduces from two to one peak.

Another general trend seems to be that reaction rates track positively with the strength of pressure induced hydrogen bond networks. However once atomic interactions fall below vdWr interaction distances the energy landscape becomes disrupted; usually a drop in combustion rate occurs

Acknowledgements

. This research was funded by the DOE Campaign-II and Joint DoD/DOE Munitions Technology Programs and performed under the auspices of the U.S. Department of Energy by Lawrence Livermore National Laboratory under contract DE-AC52-07NA27344.

References

1. Foltz, M. F., "Pressure Dependence on the Reaction Propagation Rate of PETN at High Pressure," *Proceedings of the 10th Detonation Symposium*, pp. 579-585, Boston, MA, July 1993.

2. Zaug, J. M., Young, C. E., Long, G. T., Maienschein, J. L., Glascoe, E. A., Hansen, D. W., Wardell, J. F., Black, C. K., Sykora, G. B., "Deflagration Rates of Secondary Explosives Under Static MPa-GPa Pressure," *Proceedings of the 2009 APS Shock Compression of Condensed Matter Conference*, in print, Nashville, TN, June-July 2009.

3. Foltz, M. F., "High Pressure Combustion of CL-20 Polymorphs in a Diamond Anvil Cell," *Lawrence Livermore National Laboratory Report UCRL-JC-107072 SUM&VG*, for presentation at the 1991 JANNAF CL-20 Symposium, Naval Weapons Center, China Lake, CA, April-May 1991.

4. Ciezak, J. A., Jenkins, T. A., Liu, Z., "Evidence for a High-Pressure Phase Transition of ε-2,4,6,8,10,12-Hexanitrohexaazaisowurtizitane (CL-20) Using Vibrational Spectroscopy," *Propellants, Explosives, Pyrotechnics*, Vol. 32(6), pp. 472-477, 2007.

5. Rice, S. F., and Foltz, M. F., "Very high pressure combustion: Reaction propagation rates of nitromethane within a diamond anvil cell," *Combustion and Flame*, Vol. 87, pp 109-122, 1991.

6. Montgomery, W., Zaug, J. M., Howard, W. M., Goncharov, A. F., Crowhurst, J. C., and Jeanloz, R. "Melting curve and high pressure chemistry of formic acid to 8 GPa and 600 K," *J. Phys. Chem. B*, Vol. 109, pp 19443-19447, 2005.

7. Gump, J. C., Wong, C. P., Zerilli, F. J., Peiris, S. M., "High-Pressure Structural Study of Epsilon HNIW (CL-20)," *Proceedings of the AIP Conference on the Shock Compression of Condensed Matter - 2003*, Vol. 706, pp. 963-966, 2004.

8. Russell, T. P., Miller, P. J., Piermarini, G. J., Block, S., "High-Pressure Phase Transition in γ-Hexanitrohexaazaisowurtzitane," *Journal of Physical Chemistry*, Vol. 96, pp. 5509-5512, 1992.

9. Foltz, M. F., Coon, C. L., Garcia, F., Nichols III, A. L., "The Thermal Stability of the Polymorphs of Hexanitrohexaazaisowurtzitane, Part I," *Propellants, Explosives, Pyrotechnics*, Vol. 19, pp. 19-25, 1994.

10. Bloss, F. D., "Structural Variations, Composition, and Stability," in *Crystallography and Crystal Chemistry*, p. 318, Holt, Rinehart, and Winston, New York, 1971.

11. Nielsen, A. T., Chafin, A. P., Christian, S. L., Moore, D. W., Nadler, M. P., Nissan, R .A., Vanderah, D. J., Gilardi, R. D., George, C. F., Flippen-Anderson, J. L., "Synthesis of Polyazapolycyclic Caged Polynitramines," *Tetrahedron*, Vol.54, pp. 11793-11812, 1998.

12. Raha, K., Chhabra, J. S., "Static Charge Development and Impact Sensitivity of High Explosives," *Journal of Hazardous Materials*, Vol. 34, pp. 385-391, 1993.

13. Wilson, W.H., Forbes, J. W., Liddiard, T. P., Doherty, R. M., "Sensitivity Studies of a New Energetic Formulation," *Proceedings of the AIP Conference on High Pressure Science and Technology*, pp. 1401-1404, Colorado Springs, CO, June-July 1993.

14. Ouillon, R., Pinan-Lucarré, J.P., Canny, B., Pruzan, Ph., and Ranson, P. "Raman and infrared investigations at room temperature of the internal modes behavior in solid nitromethane-h_3 and d_3 up to 45 GPa," *J. Raman Spect*., Vol. 39, pp 354-362, 2008.

15. Rahim, Z., and Barman, B. N., "Crystal physics, diffraction, theoretical and general crystallography," *Acta Crystallographica A*, Vol. 34, pp 761-764, 1978.

16. Courtecuisse, S., Cansell, F., Fabre, D., and Petitet, J. P. "Comparative Raman spectroscopy of nitromethane-h_3, nitromethane-d_3, and nitroethane up to 20 GPa," *J. Chem. Phys*., Vol. 108, pp 7350-7355, 1998.

17. Cromer, D. T., Ryan, R. R., and Schiferl, D., "The structure of nitromethane at pressures of 0.3 to 6.0 GPa," *J. Phys. Chem*., Vol. 89, pp 2315-2318, 1985.

18. Sorescu, D. C., Rice, B. M., and D. L. Thompson, "Theoretical studies of solid nitromethane," *J. Phys. Chem.*, Vol. 104, 8406-8419, 2000.

19. Yeh, C. L., and Kuo, K. K., "Ignition and combustion of boron particles," *Energy Combust. Sci.*, Vol. 22, pp 511-541, 1997.

20. Citroni, M., Datchi, F., Bini, R., Massimo, Di., Pruzan, V. P., Canny, B., and Schettino, V., "Crystal structure of nitromethane up to the reaction threshold pressure," *J. Phys. Chem. B*, Vol. 112, pp 1095-1103, 2008.

21. Hillenbrand, L. J., and Kilpatrick, M. L., "The thermal decomposition of nitromethane," *J. Phys. Chem*., Vol. 21, pp 525-535, 1953.

22. Manaa, R. M., Reed E. J., Fried, E. F., Galli, G., and Gygi, F., "Early chemistry in hot and dense nitromethane: Molecular dynamics simulations," *J. Chem. Phys*., Vol. 120, pp 10164-10153, 2004.

23. Courtecuisse, S., Fabre, D., and Petitet, J.-P., "Phase transitions and chemical transformations of nitromethane up to 350 ˚C and 35 GPa," *J. Chem. Phys*., Vol. 102, pp 968-974, 1995.

24. Pruzan, Ph., Canny, B., Power, C., and Chervin, J. C., "IR spectroscopy of nitromethane up to 50 GPa" *Proceedings of the 17th Int. Conf. on Raman Spectroscopy*, eds, Zhang, Shu-Lin, and Zhu, Bang-Fen, John Wiley & Sons, London, pp 142-143, 2000.

25. Wilson, W.H., Forbes, J. W., Liddiard, T. P., Doherty, R. M., "Sensitivity Studies of a New Energetic Formulation," *Proceedings of the AIP Conference on High Pressure Science and Technology*, pp. 1401-1404, Colorado Springs, CO, June-July 1993.

26. Constantinou, C. P., Pereira, C., and Chaundhri, M. M., "Increased concentration of the nitromethyl aci-anion in nitromethane-amine

mixtures," *Propellants, Explosives, Pyrotechnics*, Vol. 20, pp 200-205, 1995.

27. Brasch, J. W., J. Phys. Chem., "Irreversible reaction of nitromethane at elevated pressure and temperature," *J. Phys. Chem.*, Vol. 84, pp 2-84-2085, 1980.

28. Engelke, R., Schiferl, D., Storm, C. B., and Earl, W. L., "Production of the nitromethane aci ion by static high pressure," *J. Phys. Chem.*, Vol. 92, 6815-6819, 1988.

29. Shaw, R., DeCarli, P. S., Ross, D. S., Lee, E. L., and Stromberg, H. D., "Correction [Thermal explosion times of nitromethane, perdeuteronitromethane, and six dinitroalkanes as a function of temperature at static high pressures]," *Combustion and Flame*, Vol. 50, pp 123-123, 1983.

30. Winey, J. M., and Gupta, Y. M., "Shock-induced chemical changes in neat nitromethane: Uses of time-resolved Raman spectroscopy," *J. Phys. Chem. B*, Vol. 101, pp-10733-10743, 1997.

31. Wei, D. Q., Zhang, F., and Woo, T. K., "Ab initio molecular dynamics simulations of molecular collisions of nitromethane," *Shock Compression of Condensed Matter-2001*, AIP Conference Proceedings, Vol. 620, pp 407-410, 2002.

32. Dick, J. J., "Orientational-dependent explosion sensitivity of solid nitromethane," *J. Phys. Chem*., Vol. 97, pp 6193-6196, 1993.

33. Conroy, M. W., Oleynik, I. I., Zybin, S. V., and White, C. T., "Density functional theory calculations of solid nitromethane under hydrostatic and uniaxial compressions with empirical van der Waals correction," *J. Phys. Chem. A*, Vol. 113, pp 3610-3614, 2009.